0026-895X/96/020314-12$3.00/0

MOLECULAR PHARMACOLOGY, 50:314–325 (1996).

A Nonantisense Sequence-Selective Effect of a Phosphorothioate Oligodeoxynucleotide Directed against the Epidermal Growth Factor Receptor in A431 Cells

JUDY M. COULSON,[1] DAVID R. POYNER, ANDREW CHANTRY, WILLIAM J. IRWIN, and SAGHIR AKHTAR

Pharmaceutical Sciences Institute, Aston University, Birmingham, UK B4 7ET (J.M.C., D.R.P., W.J.I., S.A.), and Departments of Biochemistry and Medical Oncology, Charing Cross and Westminster Medical School, London, UK W6 8RF (A.C.)

Received December 7, 1995; Accepted May 2, 1996

SUMMARY

The overexpression of epidermal growth factor receptor (EGFr) has been implicated as a causative factor and a poor prognostic marker in a number of carcinomas. Therefore, strategies that down-regulate EGFr expression may be therapeutically useful. We designed antisense ODNs complementary to the initiation codon region of the EGFr mRNA and evaluated their efficacy in several tumor-derived cells, including the A431 cell line, that express amplified levels of EGFr. A 15-mer phosphorothioate (PS) antisense ODN (erbB1AS15) induced a concentration-dependent reduction in proliferation that was accompanied by a change in the morphology of A431 cells into more tightly clustered and discrete colonies. A 15-mer sense (PS) control oligodeoxynucleotide (ODN) and a phosphodiester (PO) version of erbB1AS15 had little or no effect on cell number or morphology, and erbB1AS15 (PS) did not induce these effects in control cell lines expressing lower levels of EGFr. The effects of erbB1AS15 (PS) on A431 cells were not mediated by a true antisense mechanism in that there was no reduction in the level of EGFr mRNA or protein over a 24-hr period, as determined by Northern and Western blotting, respectively. However, autophosphorylation of the receptor was significantly reduced by erbB1AS15 (PS) and not by control ODNs. The results of further studies suggested that this effect was mediated by a direct, dose-dependent inhibition of the EGFr tyrosine kinase enzyme and was not due to impairment of either ligand-binding or receptor dimerization. These data suggest that erbB1AS15 (PS) can inhibit proliferation and alter the morphology of A431 cells by a sequence-selective, but nonantisense, mechanism affecting receptor tyrosine kinase activity.

Antisense ODNs, in principle, have the ability to inhibit the translation of a specific transcript and thus allow targeting of an aberrant or overexpressed mRNA in a disease state. Hybridization of an ODN with the target mRNA may result in translation arrest by steric hindrance of ribosome progression or by activation of RNase H-mediated cleavage of the mRNA. Although down-regulation of the target protein has been demonstrated in a number of antisense applications (for reviews, see Refs. 1 and 2), there is, however, considerable debate as to whether many reported biological effects of ODNs are achieved by a true antisense mechanism. Indeed, the requirement for appropriate antisense controls and the problems in interpreting data from antisense experiments have recently been addressed (1, 3).

Due to the rapid degradation of PO ODNs in biological systems (4), many chemically stabilized ODNs have been synthesized. Currently, the most widely used modification is the PS backbone, and such compounds are undergoing clinical trial evaluation for therapeutic application in viral infections and leukemias (5). We have been investigating the potential use of stable PS ODNs in down-regulating overexpressed oncoproteins in brain tumors. In glioblastoma multiforme, a highly malignant brain cancer for which there is no effective therapy, the most commonly overexpressed oncogene is the c-*erbB1* gene, which encodes for EGFr (6).

EGFr is a 180-kDa protein that comprises an extracellular ligand binding domain, a transmembrane section, and an intracellular domain with protein kinase, tissue specificity, and regulatory regions (7). The external ligand binding domain is stimulated by EGF as well as by tumor growth factor-α, amphiregulin, and some viral growth factors (8). The cytoplasmic domain has tyrosine kinase activity and is autophosphorylated (9). Dimerization of the receptor is essential for the intermolecular model of activation and is suggested to involve both the kinase domain (10) and the

This project was funded by a grant from the Cancer Research Campaign.
[1] Current affiliation: Molecular Oncology Laboratories, CRC Academic Department of Clinical Oncology, City Hospital, Nottingham, UK NG5 1PB.

ABBREVIATIONS: EGFr, epidermal growth factor receptor; EGF, epidermal growth factor; ODN, oligodeoxynucleotide; mer, oligomer; PS, phosphorothioate; PO, phosphodiester; FCS, fetal calf serum; GAPDH, glyceraldehyde-3-phosphate dehydrogenase; SSC, standard saline citrate; ECL, enhanced chemiluminescence; SDS, sodium dodecyl sulfate; HEPES, 4-(2-hydroxyethyl)-1-piperazineethanesulfonic acid.

EGF binding domain (11). In addition to autophosphorylation, the activated EGFr phosphorylates many downstream molecules in a cascade response (7).

In addition to glioblastomas, abnormal EGFr expression has been reported in squamous epidermoid cancers and breast cancer (for reviews, see Refs. 7, 8, and 12). Although the EGFr gene is amplified in >40% of glioblastoma biopsies, overexpression of the EGFr is, however, lost on passage in most cell lines established from these tumors (6). The A431 cell line is derived from a vulval carcinoma and expresses the EGFr at levels 10–50-fold higher than that seen in other cell lines (13). Despite the fact that EGF can stimulate (at low concentrations) as well as inhibit (at high concentrations) the growth of these cells (14), the A431 cell line provides a simple cell culture model in which to initially evaluate ODNs directed to the EGFr, with the aim of applying the findings to malignant gliomas.

We evaluated the biological efficacy of PS and PO ODNs targeted against the initiation codon region of the EGFr mRNA in cultured A431 cells, the U87-MG glioblastoma cell line, IPFA primary astrocytes, and control HeLa cells. These cells were selected on the basis that they expressed varying levels of EGFr. In the highly expressing A431 cells, a 15-mer antisense PS ODN exhibited biological effects within 24 hr, affecting proliferation, altering colony morphology, and reducing autophosphorylation of EGFr. These effects seemed to be specific to one "antisense" sequence and most pronounced in A431 cells. Western and Northern blot analyses indicated that these biological effects were not due to an antisense mechanism of action but may be dependent on the structural conformation assumed by this "antisense" ODN.

Materials and Methods

Design and synthesis of ODNs. A number of criteria were taken into account in the design of antisense ODNs targeted to the EGFr. Potential sequences of 15 or 18 bases in length spanning the initiation codon were considered. Selection of the two antisense ODNs (Fig. 1, a and b) was based on predictions of the melting temperature, the folding, and the frequency of sites with partial matches to the ODN, within both the EGFr sequence and all other human sequences contained on the GenBank database. Computer analyses were conducted using programs from the University of Wisconsin Genetics Computer Group (15), available on the SEQNET database located at the Science and Engineering Research Council laboratory (Daresburg, UK) and accessed via Telnet. Folding of ODNs was predicted using FOLD (16), and searches for undesirable matches of ODNs were conducted against nontarget nucleotide sequences using the program FASTA (17) and within the target sequence using FindPatterns (15). Complementarity within EGFr and other human transcripts did not differ greatly between the various ODNs, so selection was made mainly on the folding criterion, as the high G/C content of the target may favor the formation of stable intramolecular structures. For both the 15- and the 18-mer antisense ODNs selected, controls corresponding to the sense version of the ODN were synthesized, along with a "nonsense" ODN, which is a scrambled form of the antisense sequence. These were checked for the potential to adopt intramolecular folding and to interact with the EGFr sequence. As the 18-mer sense ODN contained a run of four G residues, which have been implicated in the nonantisense sequence-selective activities of other ODNs (3), a third 18-mer control (erbB1con18) was synthesized, corresponding to the antisense sequence flipped in a 5′-to-3′ direction. PO and PS ODNs were synthesized on an ABI 392 automated DNA synthesizer (Applied Biosystems, Warrington, UK) using standard phosphoramidate chemical procedures and desalted on NAP10 columns (Pharmacia, Vienna, Austria). The ODN sequences synthesized and their mRNA target are shown in Fig. 1, a and b.

Stability and electrophoresis of ODNs. To determine the stability of the ODNs, 10 pmol was end-labeled with [γ-^{32}P]dATP using T4 polynucleotide kinase; unincorporated label was removed on a NENSORB 20 column (New England Nuclear-DuPont, Boston, MA) according to the manufacturer's protocol. Labeled ODNs were made up to 10 μM with the corresponding cold ODN and incubated either in 10% FCS or added to cells in serum-free medium. Samples were recovered over a time course, mixed with formamide loading buffer (80% formamide, 10 mM EDTA, pH 8.0, 1 mg/ml xylene cyanol FF, 1 mg/ml bromphenol blue), and stored at −20°. These were heated to 100° for 5 min and separated on 7 M urea/20% acrylamide gels; bands were then detected by autoradiography of wet gels. Electrophoresis of 5′ end-labeled ODNs on native 20% acrylamide gels was investigated using nondenatured ODN samples in glycerol loading buffer.

Cell culture and assays. A431 cells (a gift from Dr. P. L. Nicklin, Ciba, Horsham, UK) were maintained at 37° in a 5% CO_2 atmosphere in Dulbecco's modified Eagle's medium containing 10% FCS, 1% penicillin/streptomycin, and 2 mM glutamine (all from Life Technologies). Other cell lines used were U87-MG (purchased from the European Collection of Animal Cell Cultures, Porton Down, UK), HeLa (a gift from Dr. T. Kalamati, Institute of Cancer Research, Sutton, UK), and primary human astrocytes, IPFA (a gift from Dr. G. Pilkington, Institute of Psychiatry, London, UK), which were maintained under identical conditions in 1 mM glutamine. For experiments, cells were seeded into 24-well plates at 2.5–5.0 × 10^4 cells/well, and ODNs were added in culture medium (containing 10% FCS or serum free) 24 hr after seeding, when the cells were ~50% confluent. For proliferation assays, cells were trypsinized 24 hr after ODN addition, and the number of viable cells were counted in triplicate wells. The morphology of cells were examined by light microscopy 24 hr after the addition of ODNs, and representative replicate wells were photographed.

Western blotting and immunoprecipitation. Cells were lysed and triplicate wells were pooled, either 24 hr after the addition of ODNs or after 4 days in an alternative assay in which cells were treated with ODNs in media containing 10% FCS at 2-day intervals. For analysis of whole-cell lysates, cells were harvested in Laemmli buffer (100 mM Tris, pH 6.8, 4% SDS, 0.2% bromphenol blue, 20% glycerol, 200 mM dithiothreitol). For immunoprecipitation, cells were lysed in lysis buffer (20 mM HEPES, pH 7.5, 150 mM NaCl, 1% Triton X-100, 10% glycerol, 0.2 mM phenylmethylsulfonyl fluoride) on ice for 5 min. When cells were stimulated with EGF (50 pg/ml to 500 ng/ml), this was performed at room temperature for 10 min before lysis. Cell lysates were immunoprecipitated overnight at 4° using the anti-EGFr antibody 108 (see Ref. 18) (a gift from Dr. A. Ullrich, Max-Planck-Institute, Martinsried, Germany) and protein A-Sepharose. The immunoprecipitates were washed three times in the lysis buffer, before suspension in Laemmli buffer. Proteins prepared by whole-cell lysis or immunoprecipitation were heated to 100° for 5 min, separated on 7.5% SDS-polyacrylamide gel electrophoresis gels, and electrophoretically transferred to ECL-Hybond. Membranes were blocked using 5% nonfat dried milk in phosphate-buffered saline/Tween (0.1%). Primary antibodies used were OM-11-905 (Cambridge Research Biochemicals, Zeneca, UK) to the extracellular domain of the EGFr, 3138 (Sigma, Poole, UK) to the intracellular domain of the EGFr, and 4G10 (Upstate Biotechnology, Lake Placid, NY) to the activated receptor phosphotyrosine. An anti-actin antibody (A-2066; Sigma) was used to control for the loading of whole-cell lysates onto gels. Horseradish peroxidase-conjugated secondary antibodies, the ECL system, and ECL-Hyperfilm (Amersham International, Bucks, UK) were used for detection and autoradiography. Blots were stripped at 50° for 30 min in 100 mM 2-mercaptoethanol/2% SDS/62.5 mM Tris·HCl, pH 6.7, and blocked before being probed with an alternative primary antibody.

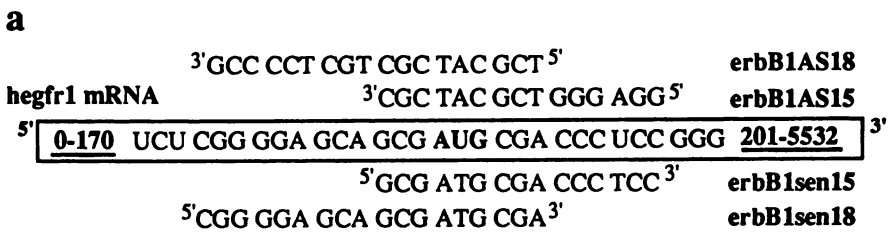

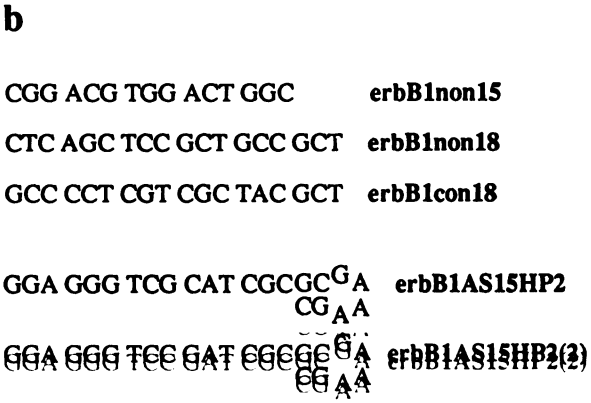

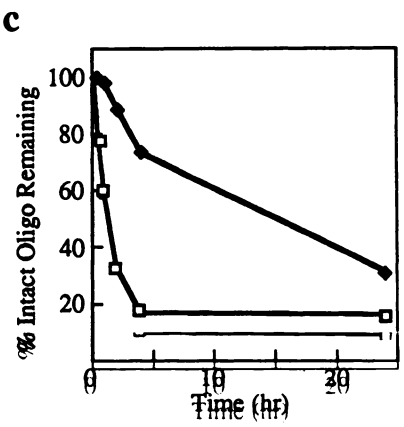

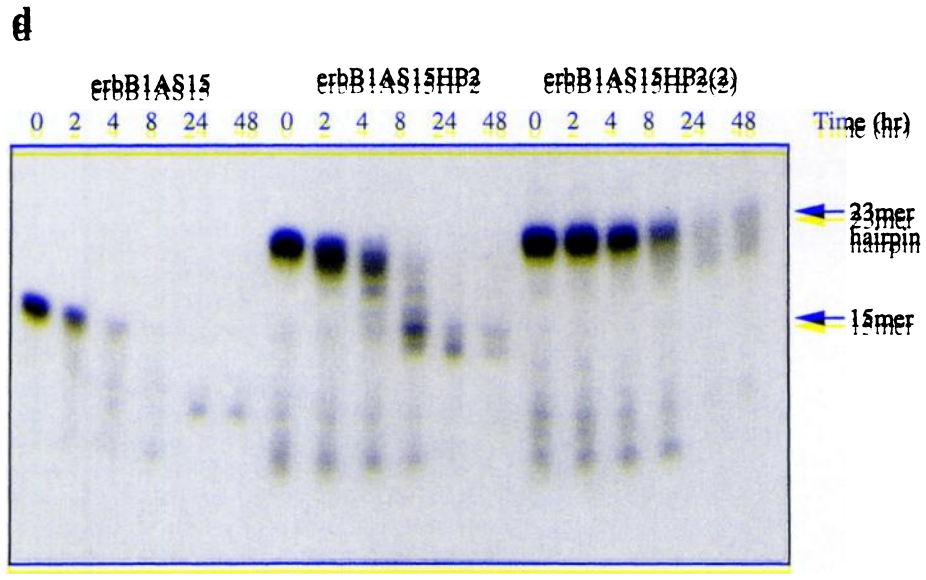

Fig. 1. The sequence and stability of ODNs directed to the initiation codon of the EGFr mRNA. a, Schematic of the region. *Bold*, initiation codon AUG. The antisense ODNs (erbB1AS15 and erbB1AS18) are shown aligned above the target sequence in a 3′-to-5′ orientation, and the corresponding sense ODNs (erbB1sen15 and erbB1sen18) are shown below in a 5′-to-3′ orientation. b, Sequence of additional ODNs. The control ODNs erbB1non15 and erbB1non18 are scrambled versions of the antisense sequences, whereas erbB1con18 is a 5′-to-3′ flipped version of erbB1AS18. ErbB1AS15HP2 is a hairpin-stabilized form of the 15-mer antisense sequence, and erbB1AS15HP2(2) is the same ODN with two base mismatches within the antisense portion. c, Representation of the degradation of the 5′ end-labeled PO (□) and PS (◆) forms of erbB1AS15 in 10% FCS, determined by densitometry of gel analysis and expressed as the percentage of intact ODN remaining with time. d, Denaturing 20% acrylamide gel showing the greater stability of 5′ end-labeled hairpin forms of erbB1AS15 (PO) in 10% FCS.

Northern blotting. Cellular RNA was prepared by lysis in 150 mM NaCl, 10 mM Tris, pH 7.4, 1 mM $MgCl_2$, and 0.5% Nonidet-P40. After centrifugation, the supernatant was extracted with Tris-buffered phenol and ethanol-precipitated. Glyoxal denatured RNA was separated on a 1.5% agarose gel and transferred to Hybond-N in 20× SSC (20 × SSC = 3 M NaCl, 0.3 M sodium citrate) overnight. The filter was baked at 80° for 2 hr, and RNA marker lanes were stained with methylene blue. Probes were used that corresponded to the 5′ end of the EGFr or to GAPDH. The human EGFr cDNA was subcloned from the plasmid pCVN-HERc (19) into the cytomegalovirus promoter-based pCMV-1 expression vector (20) (a gift from Dr. A. Ullrich, Max-Planck-Institute, Martinsried, Germany). A 1.3-kb fragment was excised by digestion with *Bam*HI. A GAPDH polymerase chain reaction product cloned into pGEM-3Z (a gift from Dr. L. Buluwela, Department of Biochemistry, Charing Cross Medical School) was excised with *Bam*HI and *Eco*RI. The required restriction

fragments were isolated from 1% low melting point agarose gels. Fifty nanograms of DNA was labeled with [α-^{32}P]dCTP by random hexanucleotide priming (ODN labeling kit; Pharmacia), and unincorporated nucleotides were removed by Sephadex G-50 spin column chromatography. Prehybridization and hybridization were carried out at 65° in the hybridization solution (6× SSC, 5× Denhardt's solution, 10 mM sodium phosphate, 1 mM EDTA, pH 8.0, 25 μg/ml denatured fragmented salmon sperm DNA). The hybridized filter was washed to an appropriate stringency (0.2× SSC/0.1% SDS). Filters were stripped for 1 hr at 65° in 50% formamide/10 mM sodium phosphate, pH 6.8, and washed three times in 2× SSC/0.1% SDS before rehybridization.

^{125}I-EGF ligand binding assays. Crude membranes were prepared from A431 cells by scraping of the cells into 1 mM EDTA/20 mM Tris, pH 7.5 (7.5 ml/75-cm^2 flask), homogenization with 12 up-and-down strokes of a pestle, and centrifugation (35,000 × *g* for 20 min). The 10-mg pellet was resuspended in 50 ml of Krebs' solution supplemented with 20 mM HEPES, HCl, pH 7.5, and 0.3% bovine serum albumin, at 0.2 mg of membrane protein/ml. Samples (0.5 ml) of membrane suspension were transferred into microcentrifuge tubes and incubated for 120 min at 37° with 10 pM ^{125}I-EGF (DuPont-New England Nuclear) and various concentrations of ODNs. Control experiments demonstrated that binding was stable and at equilibrium at this time. Incubations were terminated by centrifugation (15,000 × *g* for 5 min); the supernatant was discarded, and the pellets were washed twice with water. Membrane-bound ^{125}I-EGF was determined by γ-radiation counting.

Preparation of solubilized EGFrs. A431 cells were homogenized in 50 mM Tris, pH 7.5, 1 mM $MgCl_2$, 2 mM EDTA, 20 μg/ml soybean trypsin inhibitor, and 0.1 mM phenylmethylsulfonyl fluoride, and the membranes were spun down at 10,000 × *g* for 20 min. A crude solubilized extract was made by agitating membranes (2.5 mg/ml) in 50 mM Tris, 1% Triton X-100, 20% glycerol, 0.1% bovine serum albumin, and 0.05% sodium azide for 15 min at 4° and then centrifugation at 15,000 × *g* for 10 min. This extract was aliquoted and stored at −20°.

Assay of EGFr tyrosine kinase activity. EGFr tyrosine kinase activity was determined using the BIOTRAK EGFr tyrosine kinase enzyme assay kit according to the manufacturer's instructions (Amersham Life Sciences). Briefly, 10 μl of solubilized membranes (prepared as above) was mixed with an equal volume of substrate peptide [a model poly (tyrosine-glutamate) peptide specific for EGFr] and 5 μl of 1.2 mM ATP containing 0.05 μCi [γ-^{32}P]ATP. These were stimulated with 4 μg/ml EGF (final concentration) in the presence of ODNs for 30 min in a total volume of 33 μl. Labeled peptide was separated from unreacted [γ-^{32}P]ATP by binding to phosphocellulose filter paper and quantified by scintillation counting.

Densitometry of autoradiograms. Autoradiograms were scanned using an AGFA Focus scanner connected to a Macintosh computer, and images were saved as TIF files. The software program National Institutes of Health Image 1.58 (Division of Computing and Research Technology, National Institutes of Health, Bethesda, MD) was used to plot and quantify the band intensities using the gel-plotting macros. Values were used to calculate the half-life for ODNs and the ratio of proteins expressed from Western blots.

Results

Stability of ODNs. Two series of ODNs (15 or 18 bases long; Fig. 1, a and b) were synthesized for this study. To assess the potential degradation of these ODNs during cell culture experiments, the stability of erbB1AS15, synthesized as the PO and PS forms, was evaluated in 10% FCS over a period of 24 hr and is represented graphically in Fig. 1c. The PO ODN was rapidly degraded by 3′ exonuclease activity in 10% FCS, with a half-life of ~1 hr. However, it was determined by densitometry that 52% of the full-length erbB1AS15 (PO) was recovered after 24 hr from serum-free cell culture supernatants (data not shown), indicating that approximately half of the applied PO ODN would remain intact in the assays described below. In contrast to the PO ODN, erbB1AS15 (PS) was more stable, with a half-life of 15 hr in 10% FCS (see Fig. 1c).

The 3′ hairpin structure (HP2) in erbB1AS15HP2 is designed to protect ODNs against the action of 3′ exonuclease. Although the HP2 sequence provided a degree of protection against degradation, extending the half-life of the PO ODN to 6 hr in 10% FCS (see Fig. 1d), the strategy was less effective than previously reported for other ODNs stabilized with this sequence (21). The predicted folding for erbB1AS15HP2 revealed a potential to form an alternative low energy structure and may indicate a potential of the basic 15-mer to form intramolecular structures. To determine whether this alternative structure accounted for the poor stability of erbB1AS15HP2, a second hairpin ODN was synthesized. In erbB1AS15HP2(2), two bases in the antisense portion of the ODN have been switched; this therefore has two mismatches to the target sequence but is predicted to fold correctly into the hairpin-stabilized structure. It can be seen in Fig. 1d that this ODN was indeed more stable than erbB1AS15HP2, with a half-life of 19 hr in 10% FCS. However, these ODNs were not predominantly used in the activity studies as the antisense ODN was less stable than the PS ODN and had different stability than the mismatched ODN. Therefore, as the use of a stable ODN was preferable, PS ODNs were used in the majority of the subsequent assays.

The expression of EGFr in cell lines. It has been reported that A431 cells express 10–50-fold higher levels of the EGFr than other cell lines (13). We compared the level of EGFr protein expressed in the cell types described here by Western blotting and densitometry (data not shown). An antibody to the intracellular domain was used to detect the EGFr, and loading of gels was standardized by quantification of the level of actin detected. It was evident that the A431 epithelial cells expressed greatly amplified levels of full-length EGFr compared with the other cells. HeLa, which is also an epithelial cell line and is derived from a cervical cancer and transformed by HPV18 (22), was used as a control. HeLa cells were demonstrated to express <5% of the receptor seen in A431 cells. The IPFA astrocytes were analyzed after 10 passages in culture and showed a similar level of EGFr expression to the HeLa cell line, whereas in the glioblastoma-derived cell line, U87-MG, the level was ~15% of that in A431 cells. This represents a slight (3-fold) upregulation relative to the normal primary human astrocytes at the protein level. The level of EGFr detected in U87-MG cells is not unexpected because although it has been reported that U87-MG cells express more EGFr-specific transcripts than human fibroblasts (23), extensive overexpression of the EGFr is often lost on passage of glioma-derived cell lines (6). Therefore, the four cell types described here provide a range of EGFr expression in which to asses the biological efficacy of antisense ODNs targeted against the EGFr transcript.

The effect of ODNs on cell proliferation. To evaluate the potential of the antisense ODNs to reduce proliferation of A431 cells, an assay was undertaken based on determination of the number of viable cells at 24 hr after the addition of the ODNs. In untreated cells, the cell number increased by ~50% in serum-free medium over 24 hr. A concentration-dependent effect

of the antisense ODN erbB1AS15 (PS) was demonstrated in A431 cells, in which the cell number showed little increase from time 0 at an ODN concentration of 25 μM for both serum-free conditions (Fig. 2a) and in the presence of 10% FCS (data not shown). The PO version of erbB1AS15 did not affect the number of cells (Fig. 2a). The effect of erbB1AS15 (PS) and two 15-mer control sequences, erbB1sen15 (PS) and erbB1non15 (PS), are shown in Fig. 2b. At a concentration of 25 μM, a highly significant effect on proliferation was seen only for the antisense ODN in A431 cells. None of the 15-mer ODNs reduced cell growth of the control cell lines, U87-MG (Fig. 2c) or HeLa (Fig. 2d). The 18-mer PS antisense and control ODNs and the various hairpin-modified versions of erbB1AS15 were also evaluated in A431 cells at a concentration of 25 μM, but none of these ODNs significantly reduced proliferation (data not shown). These data therefore illustrate an antiproliferative effect that is specific to erbB1AS15 (PS) in the A431 cell line. Attempts to confirm the cell-counting data by 3-(4,5-dimethylthiazol-2-yl)-2,5-diphenyltetrazolium assays were invalidated by the morphological changes described below, as described previously in other cell types in which such alterations influence the amount of reagent internalized by the cells (24).

The effect of ODNs on cell morphology. During a microscopic examination of the cells before trypsinization in the proliferation studies described above, it was noted that the A431 cells incubated with erbB1AS15 (PS) adopted an altered colony morphology compared with the control cells. A range of ODN treatments were compared in serum-free medium (Fig. 3). A concentration-dependent effect of erbB1AS15 (PS) on the morphological appearance of A431 cells is evident in Fig. 3, b–d. This altered appearance reflected, but was not wholly attributable to, the reduction in cell number shown in Fig. 2. An altered colony morphology, apparently due to aggregation of the cells into tight clusters with few peripheral cells, was also seen. This effect was confirmed with eight independently synthesized batches of erbB1AS15 (PS). Similar results were also obtained in media containing 10% FCS (data not shown). The PO version of this ODN did not have as marked an effect on the morphology (Fig. 3e), even in serum-free medium, where it remains partially intact over the 24-hr time course. Both the 18-mer antisense and the control PS ODNs, including erbB1sen18 (which has a run of four G residues), showed little alteration in A431 colony morphology (Fig. 3i). In addition, none of the hairpin-modified forms of the antisense 15-mer ODN [erbB1AS15HP2 (PO), erbB1AS15HP2(2) (PO), or erbB1AS15HP2 (PS)] induced a morphological effect in the A431 cell line (data not shown). The effect of erbB1AS15 (PS) was demonstrated to be reversible on removal of the ODN, under serum-free conditions (Fig. 4) and in 10% FCS (data not shown). A431 cells had reverted to the normal colony morphology within 24 hr of removal of the ODN (Fig. 4d), although it is clear that the cell number is still reduced relative to that seen in the untreated cells (Fig. 4c). None of the PS ODNs investigated had an effect on the U87-MG or HeLa cell lines (data not shown). The ability of erbB1AS15 (PS) to induce morphological changes was therefore restricted to the A431 cell line, which greatly overexpressed the EGFr.

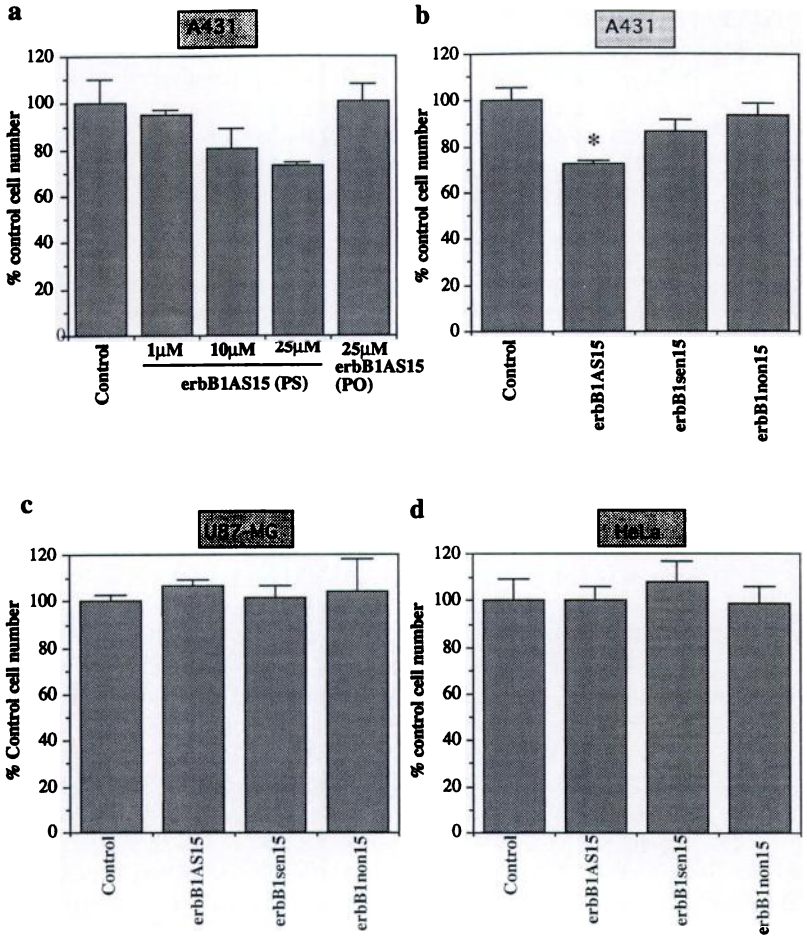

Fig. 2. The effect of ODNs on the proliferation of A431 cells and the control cell lines U87-MG and HeLa. Cell numbers were counted 24 hr after the addition of ODNs in serum-free medium to cells in 24-well plates and are expressed as a percentage of the number of untreated cells. a, Effect of a range of concentrations of erbB1AS15 on A431 cell number. b, Effect of erbB1AS15 (PS) and control PS ODNs at a concentration of 25 μM on A431 cells; the only reduction that was highly significant compared with the ODN-free control was seen with the antisense (*, $p < 0.001$). c, Effect of erbB1AS15 (PS) and control ODNs at a concentration of 25 μM on proliferation of U87-MG cells. d, the effect of erbB1AS15 (PS) and control ODNs at a concentration of 25 μM on proliferation of HeLa cells.

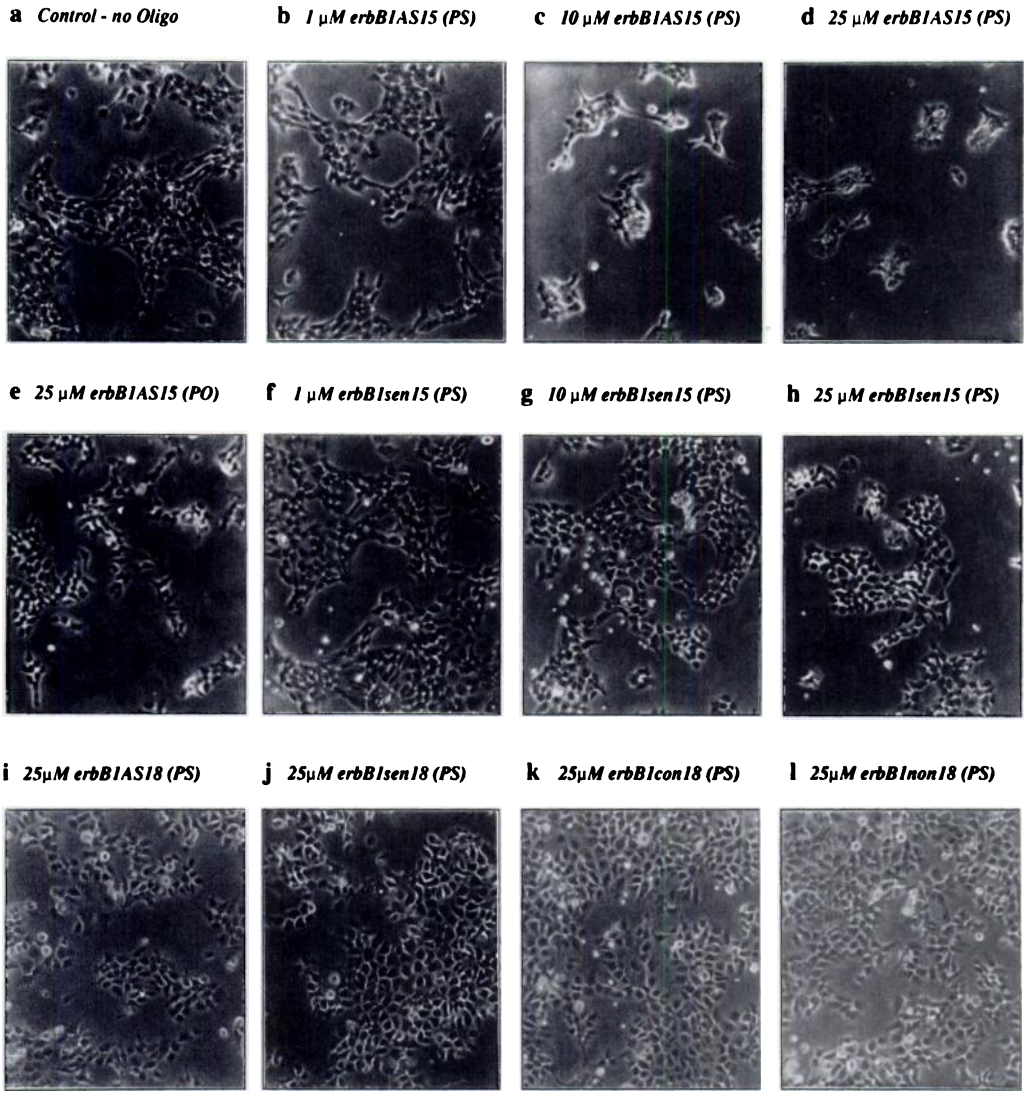

Fig. 3. Effects of ODNs on the morphology of A431 cells. The ODNs were added at the concentrations indicated to A431 cells in serum-free medium, and the cells were photographed (at a magnification of 100×) 24 hr later.

Effect of ODNs on the expression of EGFr protein and mRNA in A431 cells. The effect on cell number and colony morphology seemed to be specific to the 15-mer antisense sequence erbB1AS15 (PS), so this was further investigated at the molecular level to clarify whether a true antisense mechanism was operating. A431 cells were incubated with a range of concentrations of this ODN, with the PO antisense and the PS sense ODNs used as controls. Whole-cell lysates were made from the cells after 24 hr, separated on 7.5% SDS-polyacrylamide gel electrophoresis gels, and transferred to ECL-Hybond for Western blotting. A blot probed with an antibody to the intracellular domain of the EGFr is shown in Fig. 5a. A band of ~180 kDa was detected in all lanes, and incubation of cells with the antisense ODN did not seem to reduce the level of the protein expressed, as determined by the percentage of expression relative to actin. In further experiments, the absence of translation arrest was also demonstrated for the other ODN sequences shown in Fig. 1 (data not shown).

The level of EGFr mRNA expression was also investigated because the transcript may be depleted or cleaved if an RNase H-mediated mechanism were operating. A DNA probe to the 1.3-kb portion at the 5′ end of the EGFr sequence was produced from a clone containing the cDNA, as shown in Fig. 5b. A Northern blot of RNA isolated from cells that had been treated with either erbB1AS15 (PS) or erbB1sen15 (PS) in serum-free media for 24 hr is shown in Fig. 5c. An EGFr-specific transcript of 2.8 kb was seen in all the samples, and at long exposure times, transcripts of 5.8 and 10.5 kb were also evident. The 2.8-kb EGFr transcript, corresponding to the truncated extracellular domain of the receptor, may originate from the translocated amplified gene copy (13) or be a differential splicing product (12). The two larger transcripts are proposed to be due to differing lengths of poly(A)$^+$ tails (12), and reduction of these larger transcripts would correspond to down-regulation of the message encoding the full-length receptor. Probe of the same blot for expression of the housekeeping gene *GAPDH* confirmed equal loading of total RNA between lanes on the gel. Densitometry determined that the relative level of EGFr mRNA detected in A431 cells treated with either erbB1AS15 (PS) or erbB1sen15 (PS) was not reduced but seemed to be slightly elevated. The explanation for this is not clear, but it was demonstrated that the ODNs were not reducing the mRNA levels via an antisense-related mechanism.

An experiment was also conducted in which cells were

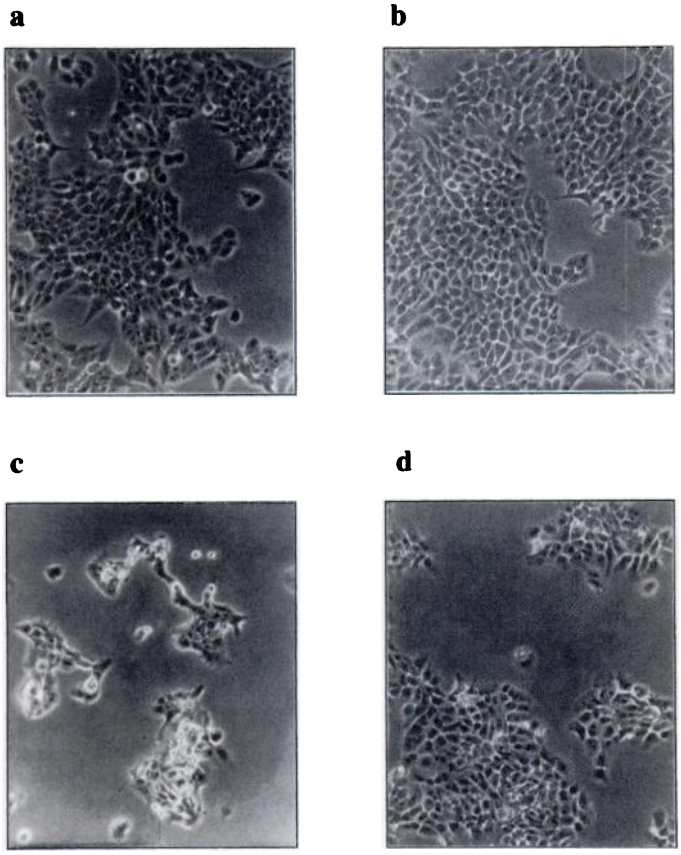

Fig. 4. Reversibility of the morphological change induced by erbB1AS15 (PS) in A431 cells. Cells were photographed (at a magnification of 100×) after incubation for 24 hr in serum-free medium in the presence or absence of the ODN. The cells were then washed and incubated in the absence of ODN in serum-free medium for 24 hr. Photographs show control cells without ODN treatment and cells after treatment with 25 μM erbB1AS15 (PS) (a and c, respectively) and after removal of the ODN and an additional 24-hr incubation (b and d, respectively).

treated with ODN for a total of 4 days in culture medium containing 10% FCS, which was replaced after 2 days (data not shown). Although this extended incubation should not be necessary to observe an antisense effect because receptor turnover occurs by internalization and degradation with a half-life of 6 hr (25), under these conditions a possible block in translation was observed. On densitometric analysis of Western blots, erbB1AS15 (PS) produced a reduction in the level of EGFr, relative to that of actin, to 54% of the control, whereas the longer antisense, erbB1AS18, caused a greater reduction, to 33% of the control. However, some of the 15- and 18-mer controls also showed a reduction, with EGFr expression ranging from 75% to 33% of the control. In contrast to the results in serum-free medium, when A431 cells were treated with these ODNs over a 4-day period in 10% FCS, the level of EGFr-specific mRNA and the ratio of the transcripts detected by Northern blotting were the same (within 10%) for the control and ODN-treated cells.

Investigation of the interaction of erbB1AS15 with the EGFr. Because an antisense-mediated block in translation of the EGFr by erbB1AS15 (PS) was not indicated, we investigated the activation of the EGFr in A431 cells. In an assay to directly determine the effect of erbB1AS15 (PS) on autophosphorylation of the EGFr, ODN-treated cells were immunoprecipitated using the anti-EGFr (108) antibody. The precipitates were separated and blotted as described for the whole-cell lysates. The antiphosphotyrosine antibody 4G10 was used to probe the blots for activated EGFr, which is autophosphorylated at tyrosine residues immediately after activation. A band of 180 kDa was detected in the control cells (Fig. 6a). The blot was stripped and reprobed with an antibody to the extracellular domain of the EGFr to determine the total level of the protein present (Fig. 6b). ODN treatment was observed to alter the level of activation; this was quantified by densitometry, and the ratio of phosphotyrosine to EGFr was determined. Autophosphorylation of the receptor in erbB1AS15 (PS)-treated A431 cells was reduced to 17% of the level in the untreated cells. The sense ODN also reduced the level of autophosphorylation but to a lesser extent than erbB1AS15 (PS). In contrast, the nonsense sequence did not significantly affect the level of activation of the receptor.

Further experiments were conducted to confirm this interference of erbB1AS15 (PS) in EGFr autophosphorylation. The histogram in Fig. 6c illustrates an experiment with three separate replicates for each treatment. Using the Student's *t* test, a statistically significant reduction in the phosphotyrosine-to-EGFr ratio was produced by 50 μM erbB1AS15 (PS) ($p < 0.02$). In general, a reduction in autophosphorylation to ~30% of the control levels was observed after culture in the presence of 25 μM erbB1AS15 (PS) under serum-free conditions or in 10% FCS (data not shown), although stimulation of the cells with 500 pg/ml EGF immediately before immunoprecipitation resulted in a reduction to only ~75% of the control level. It was therefore demonstrated that erbB1AS15 (PS) was altering the level of basal activation rather than the level of expression of the EGFr.

Ligand-binding assays were carried out to determine whether this interference in activation of the EGFr was a result of competition by the ODN for the EGF binding site on the receptor. A summary of the effect of ODNs, in the 25–50 μM concentration range, on ligand binding is given in Table 1, and it was demonstrated that this was not the mechanism of action. None of the ODNs tested, including erbB1AS15 (PS) and a PS ODN directed to the c-*myc* initiation codon containing a run of four G residues, reduced binding of ^{125}I-EGF to isolated A431 membranes. Furthermore, gel mobility shift assays suggested that erbB1AS15 (PS) did not bind directly to the EGF ligand either (data not shown). Using the method of Zhou *et al.* (40), we also found that this ODN was not interfering with *in situ* EGFr dimerization in A431 cells (data not shown). It therefore seems that erbB1AS15 (PS) operates via a nonantisense mechanism, inhibiting activation of the EGFr in a manner that is noncompetitive for the EGF ligand or its binding site and does not interfere with receptor dimerization.

EGFr tyrosine kinase activity. In an attempt to examine whether erbB1AS15 (PS) could directly interfere with the receptor tyrosine kinase enzyme activity, we investigated this in solubilized receptor preparations of A431 cells. Stimulation of solubilized EGFrs with EGF at a supramaximal concentration resulted in a control rate of incorporation of P_i of 26 ± 2 pmol min^{-1} and is shown as the control tyrosine kinase enzyme activity in Fig. 7. Incubation with 25 μM erbB1non15 (PS), a scrambled control ODN, did not affect EGFr tyrosine kinase activity. However, erbB1AS15(PS) ex-

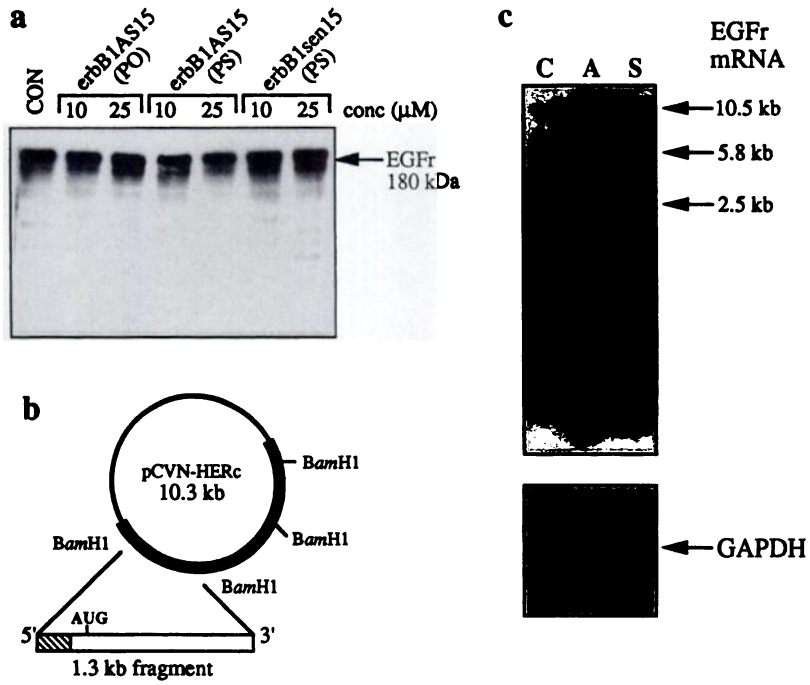

Fig. 5. Expression of EGFr in A431 cells after the addition of ODNs. a, Western blot of whole-cell lysates from A431 cells treated with ODNs for 24 hr in serum-free conditions. The blot was probed for EGFr using the antibody 3138. *CON*, control; *conc*, concentration. b, Diagram representing the 5′ region of the EGFr DNA, which was excised as a *Bam*HI fragment from pCVN-HERc for use as a probe for Northern blotting. c, Northern blot of RNA prepared from A431 cells. *C*, Untreated cells. *A*, Cells treated with erbB1AS15 (PS). *S*, A431 cells treated with erbB1sen15 (PS) for 24 hr in serum-free medium before RNA isolation.

hibited a concentration-dependent reduction in tyrosine kinase activity (57 ± 6% and 16 ± 1% of control at 4.8 and 48 μM ODN concentrations, respectively).

Secondary structure of ODNs. The uncharacteristic folding of the HP2 form of erbB1AS15, which resulted in its unexpected rapid nuclease digestion (see above), may be an indication that this 15-mer ODN is particularly prone to the formation of intramolecular structures, which may facilitate its "aptameric" interaction with proteins such as the EGFr. Although 18- and 15-mer antisense ODNs were chosen on the basis that they were not predicted to have strong secondary structures, comparison of the electrophoretic mobility of the 15-mer PS ODNs on nondenaturing and denaturing gels (Fig. 6d) provided further evidence of ODN secondary structure formation. It can be seen that erbB1AS15 migrated faster on a nondenaturing gel than did erbB1non15, which was of the same base composition and indicates folding of erbB1AS15. A faster rate of migration was seen for the complementary sequence erbB1sen15; however, this is likely to be attributable to the base composition, as erbB1sen15 has a higher ratio of C to G residues than the antisense, which is known to increase the electrophoretic mobility of ODNs (26). In contrast, on analysis under denaturing conditions, erbB1AS15 and erbB1non15 migrated at a similar rate, whereas erbB1sen15 again electrophoresed more rapidly due to the base composition effects. In the case of the 18-mer ODNs, erbB1AS18 demonstrated little evidence of folding. The folding of erbB1AS15 into secondary structures may therefore account for the interference with EGFr tyrosine kinase activity.

Discussion

There is a growing body of evidence indicating that elevated levels of EGFr expression and the consequent induction of tyrosine kinase activity can play a pivotal role in the initiation and development of several human malignancies. Furthermore, abnormalities in EGFr expression and signaling pathways in tumors, such as brain, breast, and lung, are generally associated with increased tumor malignancy and poor patient survival (for a recent review, see Ref. 8). Thus, therapeutic strategies such as the use of antisense ODNs, which can potentially inhibit or reduce EGFr expression, are worthy of investigation as anticancer agents.

We evaluated the biological efficacy of a series of antisense and control ODNs directed against the initiation codon region of the EGFr mRNA in the squamous carcinoma A431 cell line, the U87-MG glioblastoma cell line, the well-characterized HeLa cell line, and in IPFA primary astrocytes. These human cell lines were chosen to represent tumor models with decreasing levels of EGFr expression (A431 ≫ U87-MG > HeLa and IPFA), so that a correlation among receptor expression, cell type, and ODN efficacy can be investigated.

PO, PS, and hairpin-stabilized PO ODN sequences were synthesized after careful consideration of a number of design criteria; these included assessments of the probability of self-complementarity within chosen ODN sequences and the ability of ODNs to hybridize to other sites within the EGFr mRNA and to other nontargeted mRNAs with sequences that are available from the GenBank database. The chosen ODNs, based on the above design criteria, were then evaluated for activity in cell culture. Of the two antisense and several control sequences (see Fig. 1, a and b), a 15-mer antisense PS ODN [erbB1AS15 (PS)] directed against nucleotides 183–197, which overlaps the AUG initiation codon of the human EGFr mRNA, produced the most marked biological effects. Of the cell lines used in this study, the A431 squamous carcinoma cells, which exhibit the highest expression of EGFr, were the most sensitive to this ODN sequence.

In A431 cells, the addition of erbB1AS15 (PS) produced a dose-dependent change in the morphology of these squamous epithelial cells. With an increase in erbB1AS15 (PS) concentrations from 1 to 25 μM, the appearance of the A431 cells altered dramatically from the normal morphology to more clustered discrete colonies with fewer cells. A similar effect

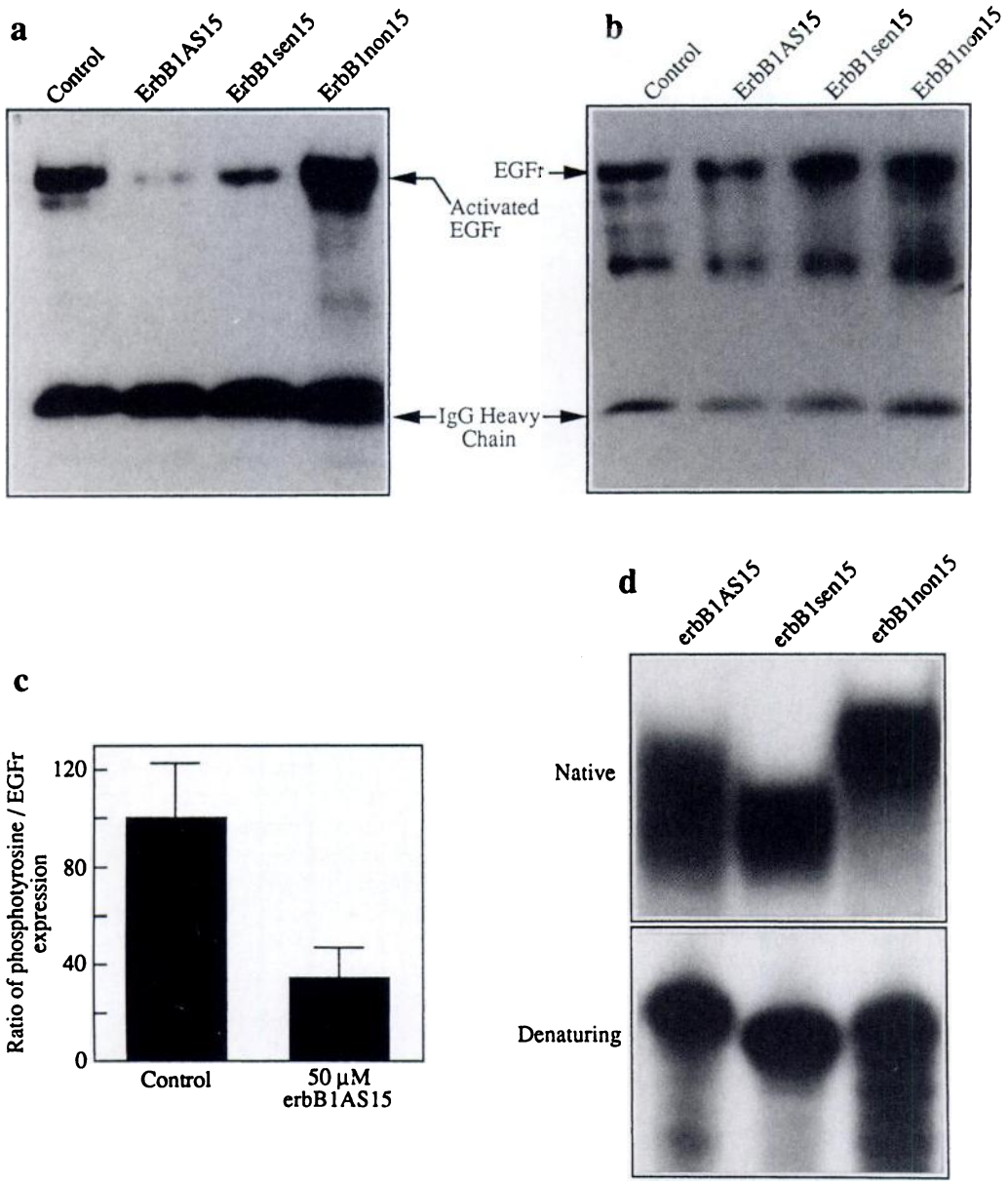

Fig. 6. Effect of ODNs on activation of the EGFr in A431 cells. a, Detection of phosphotyrosine in EGFr immunoprecipitated from A431 cells. Immunoprecipitation was carried out using the 108 antibody 24 hr after treatment of the cells with 25 μM ODN. The resultant blot was probed for the activated receptor using the 4G10 antibody. b, The same blot was probed for EGFr using the OM-11-905 antibody. c, Histogram representing the ratio of phosphotyrosine to EGFr detected in replicate experiments with untreated cells or cells treated with 50 μM erbB1AS15 (PS) (three experiments). d, Comparison of ODN migration on native and denaturing gels to illustrate the potential for formation of secondary structure; 5′ end-labeled 15-mer PS ODNs are shown.

TABLE 1

Effects of ODNs on [^{125}I]EGF binding

The ODNs were added at concentrations in the range of 25–50 μM at the time of [^{125}I]EGF addition. Values represent mean ± standard error from seven determinations. Control binding was 7.5 fmol [^{125}I]EGF/mg protein. Nonspecific binding was <5% of the total binding, and depletion of radioligand was <20%.

ODN treatment	Mean
	% of control
61 μM erbB1non15 (PS)	97 ± 6
47 μM erbB1AS15 (PO)	90 ± 7
54 μM erbB1AS15 (PS)	101 ± 2
21 μM 15mycAS (PS)	96 ± 3

was also observed, but to a much lesser extent, with a PO ODN of the same sequence as erbB1AS15 (PS), the 15-mer sense control, and an 18-mer PS antisense sequence [erbB1AS18 (PS)], which partially overlaps the erbB1AS15 target (see Fig. 1a). However, this gross morphological effect was not observed with the control ODNs, including erbB1sen18, which contains four contiguous G residues. Interestingly, this effect on morphology was also not seen in any of the other cell lines tested, including the glioblastoma-derived U87-MG and the primary astrocytic cells. The fact that the morphology of HeLa cells remained unaltered in the presence of antisense EGFr ODNs suggests that the effect is unlikely to be specific to epithelial cells but rather to the A431 cell line. This in turn suggests that the effect may be related to the elevated level of EGFr expression, which is discussed below.

The above morphological changes were also accompanied by decreased cell growth of A431 cells on erbB1AS15 (PS) ODN treatment. Data for A431 cell numbers after a 24-hr treatment with 25 μM ODN indicated a partially cytostatic effect of the 15-mer antisense ODN. This antiproliferative effect was not seen with any of the control ODNs in A431 cells or with any of the ODNs in the other cell lines.

Because only an antisense EGFr sequence was exerting these antiproliferative and morphological effects, we attempted to verify whether the sequence-selective effects of

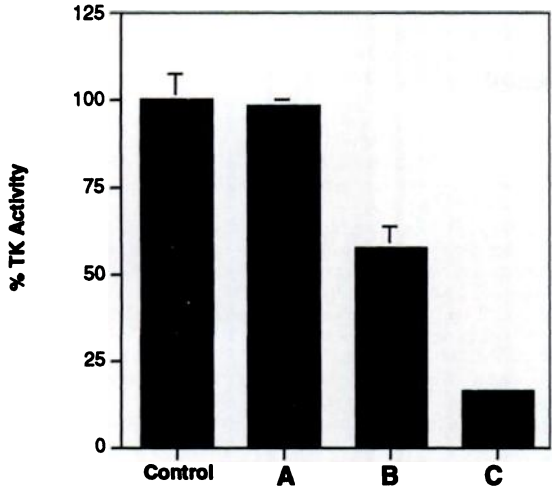

Fig. 7. Inhibition of *in vitro* EGFr tyrosine kinase activity with erbB1AS15 (PS) ODN. Solubilized EGFrs from A431 cells were stimulated with 4 μg/ml EGF, and receptor tyrosine kinase activity was determined as described in Materials and Methods. The EGF-stimulated receptor tyrosine kinase (*TK*) activity in the absence of ODNs is represented as the 100% control. *A*, Lack of inhibition with 25 μM concentration of a scrambled control [erbB1non15 (PS)]. *B and C*, Inhibition of TK activity with erbB1AS15 (PS) at 4.8 and 48 μM concentration, respectively. Data are from three to six experiments. *Error bars*, standard deviation values.

this ODN were achieved via a genuine antisense mechanism. In this regard, we determined EGFr protein levels by Western blotting for evidence of translation arrest after antisense ODN treatment. In addition, we monitored EGFr mRNA for evidence of antisense-induced RNase-mediated activity. Neither the EGFr protein or mRNA levels were reduced with either antisense or the control ODN sequences, suggesting that the observed morphological and antiproliferative effects were not due to a true antisense mechanism of action. A reduction in the EGFr protein was evident only after maintenance of A431 cells in the presence of ODNs for 4 days; however, this was not attributable to an antisense-specific mechanism, as control ODNs also had similar effects.

This is contrary to the findings of other investigators, who recently reported the use of antisense ODNs and RNA directed to the EGFr or the closely related *erb*B-2 oncogene (27–31). A reduction in *erb*B-2 was demonstrated over a 48-hr period using a PS ODN (27), but the use of a single control in these experiments is insufficient to prove an antisense mechanism (3). Interestingly, a reduction in tyrosine kinase activity was also demonstrated for this ODN, which may indicate a similar mechanism to that discussed below for erbB1AS15 (PS). An antisense effect for an EGFr stop codon-directed ODN was reported in KB cells by the use of a delivery system composed of folate/polyethylene glycol liposomes, resulting in growth inhibition, a morphological change, and reduced EGFr, whereas free ODNs were ineffective (28). Although mRNA levels were not examined, these data imply that a system to deliver free ODNs to the cytoplasm may be necessary for an antisense effect to be achieved. As free ODNs enter cultured cells through some form of endocytosis (32), they can become localized within vesicular compartments and may become nonbioavailable due to possible loss from the cell by exocytosis or even lysosomal degradation (33). Thus, it seems that antisense effects may be possible if these delivery barriers are overcome. Indeed, the intracellular expression of antisense RNA to the EGFr has also been shown to reduce EGFr expression and the malignant behavior of both KB cells (30) and the Moser human colon carcinoma cell line (31), thereby illustrating the potential efficacy of antisense mechanisms when the antisense molecule reaches the target mRNA. In addition, *in vivo*, microinjection of both antisense RNA and modified ODNs into the EGFr have been reported to modulate mouse preimplantation development in a sequence-specific manner (34). EGFr protein expression was reported to be reduced by the ODN, which incorporated the majority of the region spanned by erbB1AS15. Because the ODN was microinjected, the opportunity for extracellular interaction with the EGFr, as is likely for our ODN, was removed. It is noteworthy, however, that the use of lipofectin, a cationic liposome preparation that is thought to allow cytosolic delivery of ODNs (35), failed to enhance any antisense mechanism for erbB1AS15 (PS) in the system described here (data not shown).

It is conceivable that the accumulation of ODN-degradation products may be responsible for antiproliferative and morphological effects in A431 cells. Although this is possible for nonstabilized antisense PO ODNs (for which 50% degradation was observed during ODN treatment), the antisense erbB1AS15 (PS) sequence, which had the greatest effect, remained intact and was not degraded during the 24-hr incubation period in serum-free conditions. The effect seemed to be specific to the PS backbone in that the hairpin-stabilized PO ODN, which has a slightly increased half-life, also lacked biological activity.

To further investigate the mechanism of action for erbB1AS15 (PS), autophosphorylation of the EGFr was detected in A431 cells through the use of an immunoprecipitation assay with an antiphosphotyrosine antibody. This was shown to be inhibited in antisense [erbB1AS15 (PS)]-treated cells and, to a lesser extent, in cells treated with the corresponding sense ODN but not at all in cells treated with the 15-mer scrambled ODN. Such a mechanism may account for the effect of erbB1AS15 (PS) on cell number and morphology seen in A431 cells.

In an attempt to understand the underlying mechanism for inhibition of receptor autophosphorylation, we examined whether the PS ODN was interfering with ligand binding and receptor dimerization. Our results indicate that this effect is unlikely to be mediated by association of erbB1AS15 (PS) with the ligand or its binding site on the EGFr, as receptor/ligand binding assays did not demonstrate any competition with ^{125}I-EGF. Furthermore, the presence of the erbB1AS15 (PS) did not alter EGFr dimerization levels on stimulation with EGF (data not shown). We therefore examined the possibility that inhibition of autophosphorylation was due to a direct interaction of the ODN with tyrosine kinase activity. Studies with solubilized EGFrs showed that erbB1AS15 (PS) inhibited the enzyme in a concentration-dependent manner (see Fig. 7) and is likely to be the cause of the reduced autophosphorylation observed in intact A431 cells. Because autophosphorylation of the EGFr is an important first step in the EGF-induced signaling cascade (because it allows the docking of substrate proteins containing SH2 domains) and because the erbB1AS15 (PS) ODN caused a general inhibition of EGFr tyrosine kinase activity, there will be a major disruption of downstream signaling.

The prevention of tyrosine kinase activation was also recently reported for a PS ODN in another system (36, 37). In this case, $p210^{bcr\text{-}abl}$ autophosphorylation was inhibited in an aptameric fashion by the ODN, and this was dependent on sequence, with repeats of the motif GGC being correlated to activity (36). This effect was also seen on electroporation of the ODN into cells, and the binding site for the ODN was shown to be close to the phosphate acceptor site of the autophosphorylation domain (37). The GGC motif was not present in the erbB1AS15 sequence investigated here, suggesting that this motif is not essential for an effect. Indeed, our control nonsense sequences (erbB1non15 and erbB1non18) did contain the GGC motif but did not affect tyrosine kinase activity of EGFr. Although the exact sequence motif requirements for our system remain unknown, they are clearly different from those described by Bergan *et al*. (37).

The conformation assumed by G-rich ODNs can also influence biological activity, as is the case for a thrombin-binding ODN (38). The erbB1AS15 (PS) contains a 5′ region that is G rich (3′ GGG AGG 5′), which could potentially mediate secondary structure formation. Although computer predictions did not indicate a strong tendency for erbB1AS15 (PS) to form intramolecular structures, native gel mobility profiles suggested that some secondary structure formation was occurring that may have an important role in the nonantisense activity of this ODN.

The exact mechanism by which erbB1AS15 (PS) inhibits tyrosine kinase activity remains unclear and requires further study. It is possible that it could prevent ATP from binding or prevent the substrate complex from forming. However, it is clear that the inhibition of tyrosine kinase seen *in vitro* accounts for the inhibition of receptor autophosphorylation seen in A431 cells and the subsequent impairment of downstream signaling events involved in mediating the morphological and antiproliferative effects of erbB1AS15 (PS). It is not yet clear which cell signaling pathways downstream of EGFr autophosphorylation are involved, but likely candidates include the mitogen-activated protein kinase cascade and other targets of activated EGFr, such as phospholipase C, JAK1, and the p91STAT1 transcription factor (39).

In conclusion, we described antiproliferative and morphological effects on A431 cells that are mediated by an antisense EGFr ODN in a sequence-dependent manner but not by a true antisense mechanism. We provided evidence to suggest that these effects are mediated by inhibition of receptor tyrosine kinase activity, possibly as a result of secondary structure formation in the active ODN.

Acknowledgments

The authors wish to thank Dr. L. Buluwela for the gift of the GAPDH clone, Dr. G. Pilkington for the gift of primary astrocytes, Dr. P. L. Nicklin for the gift of A431 cells, Dr. T. Kalamati for the gift of HeLa cells, and Dr. A. Ullrich for gifts of the antibody 108 and the plasmid pCVN-HERc.

References

1. Wagner, R. Gene inhibition using antisense oligonucleotides. *Nature (Lond.)* **372:**333–335 (1994).
2. Stein, C. A., and Y. C. Cheng. Antisense oligonucleotides as therapeutic agents: is the bullet really magical? *Science (Washington D. C.)* **261:**1004–1012 (1993).
3. Stein, C. A., and A. M. Krieg. Problems in interpretation of data derived from *in vitro* and *in vivo* use of antisense oligodeoxynucleotides. *Antisense Res. Dev.* **4:**67–69 (1994).
4. Akhtar, S., R. Kole, and R. L. Juliano. Stability of antisense DNA oligodeoxynucleotide analogs in cellular extracts and sera. *Life Sci.* **49:**1793–1801 (1991).
5. Agrawal, S., and S. Akhtar. Advances in antisense efficacy and delivery. *Trends Biotechnol.* **13:**197–199 (1995)
6. Wong, A. J., P. W. Zoltlick, and D. K. Moscatello. The molecular biology and molecular genetics of astrocytic neoplasms. *Semin. Oncol.* **21:**139–148 (1994).
7. Kung, H. J., C. M. Chang, and R. J. Pelley. Structural basis of oncogenic activation of epidermal growth factor receptor, in *Biochemical and Molecular Aspects of Selected Cancers* (T. G. Pretlow and T. P. Pretlow, eds.). Vol. 2. Academic Press, San Diego, 19–45 (1994).
8. Modjtahedi, H., and C. Dean. The receptor for EGF and its ligands: expression, prognostic value and target for therapy in cancer (Review). *Int. J. Cancer* **4:**277–296 (1994).
9. Carpenter, G. Receptors for epidermal growth factor and other polypeptide mitogens. *Annu. Rev. Biochem.* **56:**881–914 (1987).
10. Chantry, A. The kinase domain and membrane localisation determine intracellular interactions between epidermal growth factor receptors. *J. Biol. Chem.* **270:**3068–3073 (1995).
11. Brown, P. M., M. T. Debanne, S. Groghe, D. Bergsma, M. Caron, C. Kay, O. Connor, and M. McCourt. The extracellular domain of the epidermal growth factor receptor: studies on the affinity and stoichiometry of binding, receptor dimerisation and a binding-domain mutant. *Eur. J. Biochem.* **225:**223–233 (1994).
12. Khazaie, K., V. Schirrmacher, and R. B. Lichtner. EGF receptor in neoplasia and metastasis. *Cancer Metastasis Rev.* **12:**255–274 (1993).
13. Ullrich, A., L. Coussens, J. S. Hayflick, T. J. Dull, A. Gray, A. W. Tam, J. Lee, Y. Yarden, T. A. Libermann, J. Schlessinger, J. Downward, E. L. V. Mayes, N. Whittle, M. D. Waterfield, and P. H. Seeburg. Human epidermal growth factor receptor cDNA sequence and aberrant expression of the amplified gene in A431 epidermoid carcinoma cells. *Nature (Lond.)* **309:**418–425 (1984).
14. Kawamoto, T., J. D. Sato, A. Le, J. Polikoff, G. H. Sato, and J. Mendelsohn. Growth stimulation of A431 cells by epidermal growth factor: identification of high-affinity receptors for epidermal growth factor by an anti-receptor monoclonal antibody. *Proc. Natl. Acad. Sci. USA* **80:**1337–1341(1983).
15. Devereux, J., P. Haeberli, and O. Smithies. A comprehensive set of sequence analysis programmes for the VAX. *Nucleic Acids Res.* **12:**387–395 (1984).
16. Zuker, M. Computer prediction of RNA structure. *Methods Enzymol.* **180:**262–288 (1989).
17. Pearson, W. R., and D. J. Lipman. Improved tools for biological sequence comparison. *Proc. Natl. Acad. Sci. USA* **85:**2444–2448 (1988).
18. Honegger, A. M., R. M. Kris, A. Ullrich, and J. Schlessinger. Evidence that autophosphorylation of solubilised receptors for epidermal growth factor is mediated by intermolecular cross-phosphorylation. *Proc. Natl. Acad. Sci. USA* **86:**925–929 (1989).
19. Riedel, H., T. J. Dull, A. M. Honegger, J. Schlessinger, and A. Ullrich. Cytoplasmic domains determine signal specificity, cellular routing characteristics and influence ligand binding of epidermal growth-factor and insulin-receptors. *EMBO J.* **8:**2943–2954 (1989).
20. Gorman, C. M., D. Gies, G. McCray, and M. Huang. The human cytomegalo-virus major immediate early promoter can be trans-activated by adenovirus early proteins. *Virology* **171:**377–385 (1989).
21. Khan, I. M., and J. M. Coulson. A novel method to stabilise antisense oligonucleotides against exonuclease degradation. *Nucleic Acids Res.* **21:**2957–2958 (1993).
22. Yee, C., I. Krishnan-Hewlett, C. C. Baker, R. Schlegel, and P. M. Howley. Presence and expression of human papillomavirus sequences in human cervical carcinoma cell lines. *Am. J. Pathol.* **119:**361–366 (1985).
23. Nister, M., C. Libermann, C. Bersholz, M. Pettersson, L. Claesson-Welsh, C. H. Heldin, J. Schlessinger, and B. Westermark. Expression of the messenger RNAs for platelet-derived growth factor and transforming growth factor-α and their receptors in human malignant glioma cell lines. *Cancer Res.* **48:**3910–3918 (1988).
24. Jabbar, S. A. B., P. R. Twentyman, and J. V. Watson. The MTT assay underestimates the growth inhibitory effects of interferons. *Br. J. Cancer* **60:**523–528 (1989).
25. King, A. C., R. A. Willis, and P. Cuatrecasas. Accumulation of epidermal growth factor within cells does not depend on receptor cycling. *Biochem. Biophys. Res. Commun.* **97:**840–845 (1980).
26. Frank, R., and H. Koster. DNA chain length markers and the influence of base composition on electrophoretic mobility of oligodeoxyribonucleotides in polyacrylamide gels. *Nucleic Acids Res.* **6:**2069–2087 (1979).
27. Brysch, W., E. Magal, J. C. Louis, M. Kunst, I. Klinger, R. Schlingensiepen, and K. H. Schlingensiepen. Inhibition of $p185^{c\text{-}erbB\text{-}2}$ proto-oncogene expression by antisense oligodeoxynucleotides down-regulates p185-associated tyrosine-kinase activity and strongly inhibits mammary tumour-cell proliferation. *Cancer Gene Therapy* **1:**99–105 (1994).
28. Wang, S., R. J. Lee, G. Cauchon, D. G. Gorenstein, and P. S. Low. Delivery of antisense oligodeoxyribonucleotides against the human epidermal

growth factor receptor into cultured KB cells with liposomes conjugated to folate via polyethylene glycol. *Proc. Natl. Acad. Sci. USA* **92**:3318–3322 (1995).
29. Okada, T., K. Yamaguchi, and J. Kamashita. Triplex-forming oligonucleotide binding represses transcription of the human c-*erb*B gene in glioma. *Growth Factors* **11**:259–270 (1994).
30. Moroni, C. M., M. C. Willingham, and L. Beguinot. EGF-R antisense RNA blocks expression of the epidermal growth factor receptor and suppresses the transforming phenotype of a human carcinoma cell line. *J. Biol. Chem.* **267**:2714–2722 (1992).
31. Chakrabarty, S., S. Rajagopal, and S. Huang. Expression of antisense epidermal growth factor receptor RNA down-modulates the malignant behaviour of human colon cancer cells. *Clin. Exp. Metastasis* **13**:191–195 (1995).
32. Akhtar, S., and R. L. Juliano. Cellular uptake and intracellular fate of antisense oligonucleotides. *Trends Cell Biol.* **2**:139–144 (1992)
33. Hudson, A. H., W. Lee, J. Porter, J. Akhtar, R. Duncan, and S. Akhtar. Stability of antisene oligonucleotides during incubation with a mixture of isolated lysosomal enzymes. *Int. J. Pharm. (Amst.)* **133**:257–263 (1996).
34. Brice, E. C., J. X. Wu, R. Muraro, E. D. Adamson, and L. M. Wiley. Modulation of mouse preimplantation development by epidermal growth factor receptor antibodies, antisense RNA and deoxyoligonucleotides. *Dev. Genet.* **14**:174–184 (1993).
35. Bennett, C. F. Intracellular delivery of oligonucleotides with cationic liposomes, in *Delivery Strategies for Antisense Oligonucleotide Therapeutics* (S. Akhtar, ed.). CRC Press, Boca Raton, 223–232 (1995).
36. Bergan, R., Y. Connell, B. Fahmy, E. Kyle, and L. Neckers. Aptameric inhibition of $p210^{bcr\text{-}abl}$ tyrosine kinase autophosphorylation by oligodeoxynucleotides of defined sequence and backbone structure. *Nucleic Acids Res.* **22**:2150–2154 (1994).
37. Bergan, R., E. Kyle, Y. Connell, and L. Neckers. Inhibition of protein-tyrosine kinase activity in intact cells by the aptameric action of oligodeoxynucleotides. *Antisense Res. Dev.* **5**:33–38 (1995).
38. Tsiang, M., C. S. Gibbs, L. C. Griffin, K. E. Dunn, and L. L. K. Leung. Selection of a suppressor mutation that restores affinity of an oligonucleotide inhibitor for thrombin using *in vitro* genetics. *J. Biol. Chem.* **270**: 19370–19376 (1995).
39. Wright, J. D., W. M. Reuter, and M. J. Weber. An incomplete program of cellular tyrosine phosphorylations induced by kinase defective epidermal growth factor receptors. *J. Biol. Chem.* **270**:12085–12093 (1995).
40. Zhou, Q., S. Hakomori, K. Kitamura, and Y. Igarashi. GM_3 directly inhibits tyrosine phosphorylation and de-N-acetyl-GM_3 directly enhances serine phosphorylation of epidermal growth factor receptor, independently of receptor-receptor interaction. *J. Biol. Chem.* **269**: 1959–1965 (1994).

Send reprint requests to: Dr. Saghir Akhtar, Department of Pharmaceutical and Biological Sciences, Aston University, Aston Triangle, Birmingham, B4 7ET, UK. E-mail: s.akhtar@aston.ac.uk